

## Research Article

# Hesperitin Synergistically Promotes the Senescence Induction of Pentagamavunone-1 in Luminal Breast Cancer Cells, T47D

Fauziah Novita Putri Rifai<sup>1,2</sup>, Mila Hanifa<sup>2</sup>, Ummi Maryam Zulfin<sup>2</sup>, Muthi Ikawati<sup>2,3</sup>, Edy Meiyanto<sup>2,3\*</sup>

1) Master of Biotechnology Study Program, Graduate School, Universitas Gadjah Mada, Yogyakarta 55281, Indonesia

2) Cancer Chemoprevention Research Center, Faculty of Pharmacy, Universitas Gadjah Mada, Yogyakarta 55281, Indonesia

3) Macromolecular Engineering Laboratory, Department of Pharmaceutical Chemistry, Faculty of Pharmacy, Universitas Gadjah Mada, Yogyakarta 55281, Indonesia

\* Corresponding author, email: edy\_meiyanto@ugm.ac.id

### Keywords:

Curcumin analog

Hesperitin

Senescence

Synergistic effect

T47D cells

### Submitted:

23 August 2023

### Accepted:

03 November 2023

### Published:

04 March 2024

### Editor:

Ardaning Nuriliani

### ABSTRACT

Pentagamavunone-1 (PGV-1), a curcumin analog, is a promising anticancer candidate for several cancers that have been proven *in vitro* and *in vivo*. However, the efficacy of PGV-1 against breast cancer is subject to improvement to achieve a more suitable application. Here we propose hesperitin, a citrus flavonoid, to increase the anticancer potency of PGV-1 in luminal breast cancer cells. We use the T47D cell as the model to investigate the effect of co-administration of PGV-1 and hesperitin on cell cycle block, apoptosis modulation, and senescence phenomena. PGV-1 and hesperitin showed strong and weak cytotoxicity with an IC<sub>50</sub> value of 2 μM and 100 μM, respectively. The co-treatment of PGV-1 and hesperitin resulted in strong synergistic effects with combination index (CI) value of ≤ 0.2. This combination caused apoptosis in correlation with cell cycle disruption in G2/M phase at 48 h. In particular, PGV-1 and hesperitin combination increased the incidence of cellular senescence significantly higher than the single treatment. Despite its senescence potentiation, hesperitin did not induce senescence in normal cells. Taken together, hesperitin may increase the anticancer potency of PGV-1 by modulating cell cycle arrest and apoptosis via the senescence mechanism.

Copyright: © 2024, J. Tropical Biodiversity Biotechnology (CC BY-SA 4.0)

### INTRODUCTION

Luminal breast cancer therapy remains a major challenge in oncology (Masoud & Pagès 2017). In addition to the complexity of the cellular physiology of cancer, there is also the emergence of resistance to specific targeted drugs (Baghban et al. 2020). Tamoxifen and its analogs are an example of a chemotherapeutic agent with a specific target, namely the estrogen receptor (ER) which is then referred to as an ER antagonist (Burstein 2020). Long-term use of ER antagonists can cause cancer cell resistance because cancer cells will divert their growth signal to the MAPK pathway (Clusan et al. 2023). In this case, the growth of cancer cells will not depend on ER signals anymore. Diversion of this pathway also occurs in the use of aromatase inhibitor drugs which causes a decrease in their effectiveness (Heery et al. 2020). Therefore, luminal breast

cancer therapy still requires other specific targeted agents. The application of agents that target DNA (e.g. doxorubicin) or microtubules (e.g. taxol) is an option, but there are still problems with side effects that make the patient's condition worse (Čermák et al. 2020). To overcome this problem, the finding of drugs that are safer but effective for luminal breast cancer is taken as a challenge.

Our group has developed a prospective anticancer agent, called Pentagamavunone-1 (PGV-1). This compound exhibits high cytotoxic activities against luminal breast cancer and triple negative breast cancer (TNBC) (Meiyanto & Larasati 2019; Utomo et al. 2022). In the xenograft model, PGV-1 also shows significant effect of tumor growth suppressor activity against several types of cancer, such as TNBC and leukemia (Lestari et al. 2019). Interestingly, the tumor growth inhibition ability of PGV-1 is comparable to that of standard drugs (Meiyanto et al. 2019). Moreover, PGV-1 did not show any significant side effects (Novitasari et al. 2021). Due to its potential anti-cancer characteristics, PGV-1 holds promise for future development as a chemotherapy treatment.

The distinctive ability of PGV-1 to impede the growth of cancer cells lies in its cleverness, specifically by hindering the process of mitosis during prometaphase (Lestari et al. 2019). However, the performance of PGV-1 as an anticancer still needs to be improved to gain more effectiveness to suppress tumor cell development. One strategy is to apply in combination with chemopreventive agents that can increase their cytotoxic effect on cancer cells synergistically (Hasbiyani et al. 2021; Musyayyadah et al. 2021; Endah et al. 2022). Chemopreventive agents are compounds that have weak tumor growth inhibiting properties through inhibition of growth signals, for example MAPK inhibitors (Haque et al. 2021). These compounds can be expected to support the cytotoxic properties of other anticancer compounds with different targets.

Those compounds that potentially act as MAPK inhibitors are mostly flavonoid substances, including ones that are largely found in citrus (Meiyanto et al. 2012). So far, there are several citrus flavonoid compounds that have been applied in combination with chemotherapeutic agents to suppress cancer growth, including the co-treatment with PGV-1 in some types of cancer cells. The results of all studies on the combination of flavonoids with chemotherapeutic agents synergistically increase their cytotoxic effects. For example, diosmin with PGV-1 synergistically enhances their cytotoxicity through modulation of senescence and mitotic catastrophe in TNBC 4T1 cells (Musyayyadah et al. 2021). Diosmin also enhances the cytotoxicity of PGV-1 in colon cancer cells (Ikawati et al. 2023). In accordance to those findings, the combination of a chemotherapy agent doxorubicin with hesperidin and its aglycone form, hesperitin, synergistically inhibits the migration of 4T1 and MCF7/HER2 cells (Nurhayati et al. 2020; Amalina et al. 2023). Both hesperidin and hesperitin have great potential to amplify the cancer-preventive efficacy of PGV-1 within breast cancer cells.

Hesperidin and hesperitin are two major methoxy flavonoids of *Citrus* sp. that are considerably safe to normal cells (Putri et al. 2022). They are selectively cytotoxic toward cancer cells but not toxic in normal cells (Filho et al. 2021; Choi et al. 2022). Even though showing similar bioactivities, the bioavailability of these two compounds remains critical in considering the best one as a co-chemotherapeutic agent. Hesperidin has lower bioavailability than hesperitin (Wdowiak et al. 2022). The low bioavailability of hesperidin in systemic circulation is due to the presence of the rutinoside sugar group attached to the flavonoid (Crescenti et al. 2022). Moreover, oral hesperidin undergoes first pass metabolism

(Corrêa et al. 2019). Hesperidin must be deglycosylated into hesperitin before it has the capability to be taken in by the intestine (Corrêa et al. 2019). Intestinal enterobacteria release  $\alpha$ -rhamnosidase and  $\beta$ -rhamnosidase that will cleave the rutinose sugar group in hesperidin into its aglycone (Mueller et al. 2018). Meanwhile, hesperitin can passively diffuse into the blood to obtain optimal bioavailability (Takumi et al. 2012; Wdowiak et al. 2022). Thus, the approach to exploring the potential of co-chemotherapeutic agents from the citrus flavonoid hesperitin has a more promising potential in the future.

We previously investigated hesperidin in combination with PGV-1. In this study, we focused on investigating the synergistic effect of applying combination treatment hesperitin and PGV-1 on luminal breast cancer cells. We used T47D as a model that represents ER expressing breast cancer cell lines. This cell line is also known to express PgP that facilitates efflux of some chemotherapeutic drugs resulting in resistance phenomenon (Lee & Choi 2022). Swiss Prediction analysis, fortunately shows that PGV-1 is not subjected to be the substrate of PgP. However, hesperitin shows inhibitory effects on the MAPK/Akt pathway to induce autophagy and apoptosis that might contribute to growth inhibitory effect of PGV-1 on T47D cells (Lin et al. 2023). Our primary aim is to assess the ability of hesperitin to augment the efficacy of PGV-1, particularly in luminal breast cancer. Additionally, we aim to explore the impact of combining these two compounds on the phenomenon of cell death.

## **MATERIALS AND METHODS**

### **Ethical approval**

Authorization for all research procedures was granted by the Medical and Health Ethical Committee of the Faculty of Medicine, Public Health and Nursing, Universitas Gadjah Mada (No. KE/FK1012/EC/2020).

### **Chemicals**

Cancer Chemoprevention Research Center (CCRC), Faculty of Pharmacy, Universitas Gadjah Mada was provided PGV-1 with purity HPLC 95% (Utomo et al. 2022). Hesperitin (HST) was obtained from Sigma Aldrich (No. Cat. W431300-5G).

### **Cell culture**

T47D cells, NIH-3T3 cells, and Vero cells were cultured in Dulbecco's Modified Eagle's Medium (DMEM) high glucose (Gibco), enriched with 10% fetal bovine serum (FBS) (Gibco), and 1% Penicillin-Streptomycin (Gibco). This cultivation was carried out in an incubator at 37°C with a 5% CO<sub>2</sub> atmosphere. The cells were collected using 0.25% Trypsin-EDTA (Gibco) when they reached approximately 80% confluence.

### **Trypan blue exclusion assay**

Cultures of T47D cells ( $5 \times 10^4$  cells/well) were established in 24-well plates and allowed to incubate for one night. Cells were treated with 0.5-16  $\mu$ M PGV-1, 15-1000  $\mu$ M HST, or their combinations. After 24 h incubation, the cells were rinsed using 500  $\mu$ L of phosphate buffer saline (PBS) 1 $\times$ , followed by the addition of 100  $\mu$ L of 0.25% trypsin-EDTA per well for a duration of 3 min. Cell suspension (10  $\mu$ L) was treated with 10  $\mu$ L of trypan blue 0.4%. Cells devoid of color were considered viable cells, while cells displaying a blue hue were regarded as dead cells. Viable and overall cell counts were performed within each well using an inverted microscope (Olympus). The percentage of cell viability was derived from the ratio of viable cells to total cells. This metric was utilized to compute

IC<sub>50</sub> and CI values across three separate experiments, each conducted in triplicate (Musyayyadah et al. 2021).

### MTT Assay

NIH-3T3 and Vero cells ( $1 \times 10^4$  cells/well) were introduced into 96-well plates and allowed to incubate overnight. Following this, the cells were exposed to varying concentrations of HST (ranging from 1  $\mu$ M to 500  $\mu$ M) for a duration of 24 h. Subsequently, the cells underwent a PBS wash, and a solution comprising 100  $\mu$ L of 0.5% 3-(4,5-dimethylthiazol-2-yl)-2,5-diphenyltetrazolium bromide (MTT) (Sigma) in PBS 1 $\times$  was added, followed by a 4 h incubation period. Once the conversion of tetrazolium salts to blue formazan crystals was complete, as denoted by their visible presence, 100  $\mu$ L of 10% sodium dodecyl sulfate (SDS) stopper was introduced, and the cells were left to incubate overnight. The measurement of absorbance at 595 nm was performed using an ELISA reader (Bio-Rad) (Hanifa et al. 2022).

### Measuring cell cycle profile

T47D cells ( $2 \times 10^4$  cells/well) were cultured in 6-well plates and left to incubate overnight. Following this, cells underwent treatment with PGV-1 at concentrations of 0.5 and 1  $\mu$ M, HST at concentrations of 25 and 50  $\mu$ M, as well as their combination, for a duration of 24 h. After treatment, the cells were subjected to a wash with 500  $\mu$ L of PBS 1x, followed by detachment using 0.25% trypsin-EDTA for a 3 min interval. To deactivate the enzyme, 1 mL of culture medium was introduced, and the cells were gathered, subsequently undergoing a rinse with 500  $\mu$ L of cold PBS 1x. Centrifugation at 600 rpm for 5 min facilitated the removal of the supernatant, after which the pellet cells were fixed using 500  $\mu$ L of 70% alcohol, and this was done at room temperature for a span of 30 min, followed by another 5-min centrifugation. The pellet cells then underwent a wash with 500  $\mu$ L of PBS 1x, once again followed by centrifugation. Subsequently, the resulting cells were stained with a solution composed of 1 mg/ml propidium iodide (Merck), 10 mg/mL RNase (Merck), Triton-X 100 at a volume of 1 (Merck), and PBS 1x. Cell distribution across the SubG1, G0/G1, S, and G2/M phases, indicative of DNA content, was assessed utilizing Flow Cytometry (BD Biosciences Accuri C6) alongside BD Accuri C6 Software (Amalina et al. 2023).

### Measuring apoptosis

T47D cells ( $2 \times 10^4$  cells/well) were cultivated within 6-well plates and left to incubate overnight. Subsequently, the cells were subjected to treatment with either PGV-1 or HST separately, as well as in combination, for durations of 24 and 48 h. Following treatment, the cells underwent a wash with 500  $\mu$ L of PBS 1x, and then were detached utilizing 0.25% trypsin-EDTA for a span of 3 min. The enzyme reaction was deactivated through the introduction of 1 mL of culture medium, after which the cells were gathered. Centrifugation at 600 rpm for 5 min was performed, resulting in the removal of the supernatant. The pellet cells were subsequently exposed to 100  $\mu$ L of binding buffer, 5  $\mu$ L of FITC Annexin V, and 5  $\mu$ L of propidium iodide (PI) (at a concentration of 50  $\mu$ g/mL) for a 5 min interval. Analysis using Flow Cytometry (BD Biosciences Accuri C6) in conjunction with BD Accuri C6 Software was employed to discern between live, apoptotic, and necrotic cells (Amalina et al. 2023).

### Measurement of senescent cells

All cell models (T47D, NIH-3T3, and Vero cells) were grown in the concentration of 1, 2, and 2, respectively  $10^4$  cells/well into 6-well plates and

allowed to incubate overnight. After incubation with the drugs for 24 h, the cells underwent a PBS 2× pH 6.0 rinse, followed by fixation using a 4% paraformaldehyde solution for 10 min. Subsequent washing was carried out twice with 1× PBS, followed by staining using a 1 mL X-gal solution. Following an incubation period of 72 hours, the cells were assessed under an inverted microscope at 200× magnification, and enumeration was conducted using ImageJ Software (Salsabila et al. 2023).

**Data analysis**

The gathered experimental data underwent analysis through SPSS 25 (SPSS Inc., Chicago, IL, USA, version 25). One-way ANOVA was implemented to assess distinctions between groups and an independent sample *t*-test was used to ascertain differences between individual samples. Following that, the Bonferroni test was employed in conjunction with one-way ANOVA, with considering significance at a level of *p* < 0.05.

**RESULTS**

**Growth inhibitory effects of PGV-1 and HST on T47D cells**

We assessed the cytotoxic characteristics of PGV-1, HST, and their combined effect on T47D luminal breast cancer cells through the trypan blue exclusion assay. First, we performed a single cytotoxic assay using PGV-1 and HST in T47D cells for 24 h. We found that both PGV-1 and HST exhibited cytotoxic properties, with IC<sub>50</sub> values of 2 μM and 100 μM, respectively (Figure 1a and 1b). These results indicate that PGV-1 shows strong cytotoxic activity, whereas HST has a weak cytotoxic effect on T47D cells. Thus, PGV-1 has a stronger inhibitory effect on cell growth than HST does (*p* < 0.001).

Next, we combined the growth suppression properties of PGV-1 and HST against T47D at different concentrations of PGV-1 0.25 μM, 0.5 μM, 1 μM and HST 12.5 μM, 25 μM, 50 μM. Interestingly, HST in-

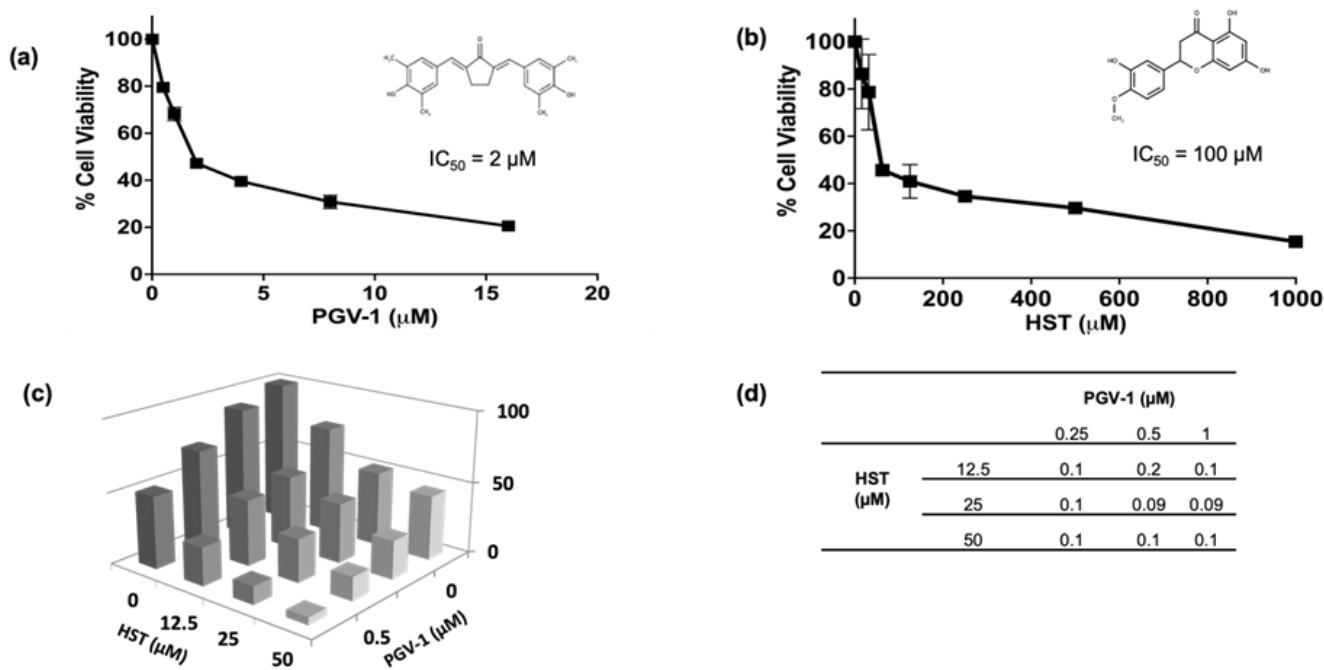


**Figure 1.** Growth suppression properties of PGV-1, HST, and their co-administration in T47D cells. Cells were subjected with PGV-1 (a), HST (b), or their co-administration (c). The concentrations of PGV-1 and HST used in the combination were based on IC<sub>50</sub> value, which are PGV-1 0.25 μM, 0.5 μM, 1 μM and HST 12.5 μM, 25 μM, 50 μM, respectively. Cell viability and CI value (d) are expressed as the mean ± standard error (SE) for a total of three replicates.

creased the efficacy of PGV-1 synergistically with CI values  $\leq 0.2$  (Figure 1c and 1d). The combination of PGV-1 and HST is believed to have good prospects as a chemotherapeutic agent. Thus, we used the combined cytotoxic assay concentrations of PGV-1 and HST for further testing on cell cycle, apoptosis, and cellular senescence effects.

### Effect of PGV-1 and HST on cell cycle profile

To investigate the impact of combining HST and PGV-1 in restraining cancer cell growth, we examined the influence of HST and PGV-1 individually and in co-administration on hindering the progression of cell cycle. HST and PGV-1 showed cell cycle arrest phenomenon in 24 h incubation time. In this case, PGV-1 0.5 and 1  $\mu\text{M}$  exert cell cycle inhibition especially at G2/M phase by 33% and 34% (Figure 2,  $p < 0.05$ ). A comparable outcome was likewise witnessed in the examinations involving HST concentrations of 25 and 50  $\mu\text{M}$ , resulting in a 31% adjustment in cell cycle inhibition at the G2/M phase (Figure 2). Additionally, the co-administration application of all doses of HST and PGV-1 led to cell cycle inhibition within the G2/M phase (Figure 2). Notably, the co-administration of HST at 50  $\mu\text{M}$  and PGV-1 at 0.5  $\mu\text{M}$  exhibited the most substantial cell cycle inhibition in the G2/M phase among the various concentrations, particularly within T47D. Halting the cell cycle progression at the G2/M phase prompts cancer cells to cease their proliferation and eventually undergo cell death. Nevertheless, additional verification is necessary to substantiate the collaborative impact of the two compounds on inducing cancer cell demise.

### Effect of PGV-1 and HST on apoptosis induction

To validate the impact of HST, PGV-1, and their co-administration ap-

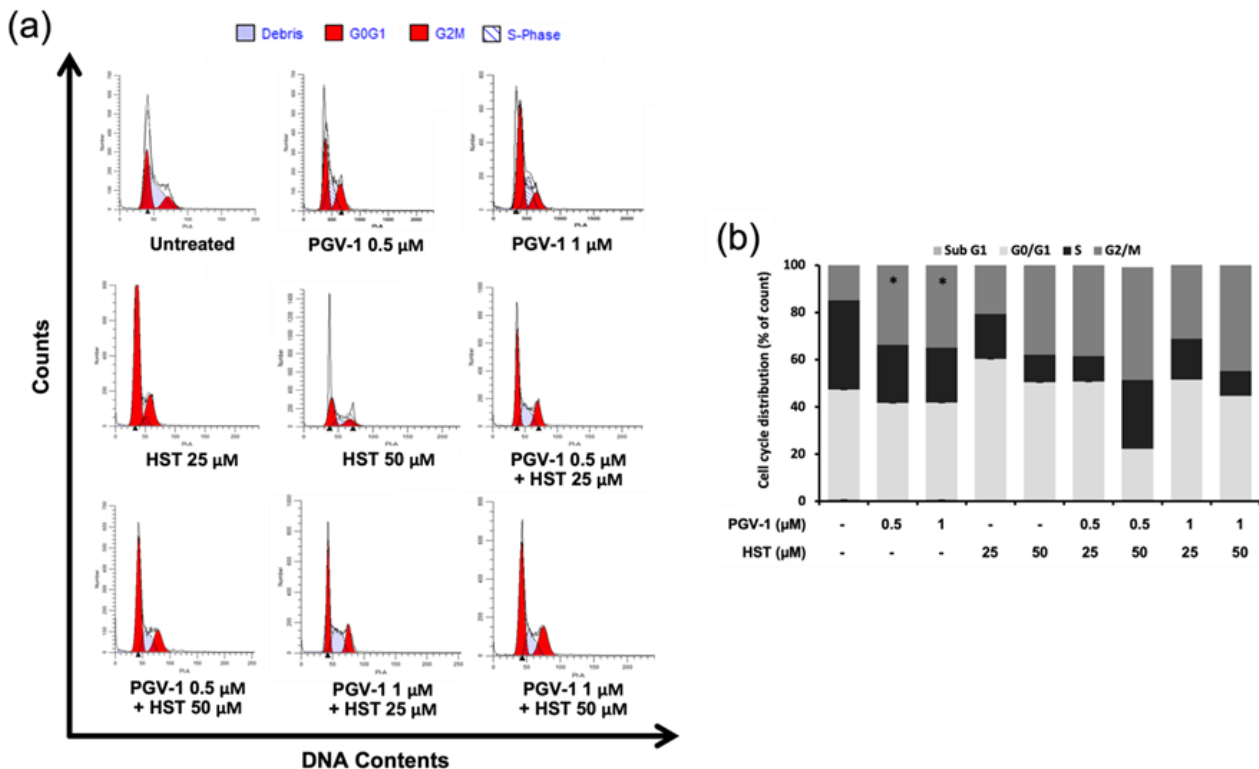


**Figure 2.** Cell cycle profile after treatment with PGV-1, HST, and their co-administration on T47D. Cells were subjected with PGV-1, HST, or both co-administration in various concentrations as indicated followed by 24 h incubation. After washing with PBS, the cells were stained with propidium iodide and then subjected to flow cytometry. Cell cycle profile were generated from flow cytogram (a) into quantitative diagram (b) to obtained the significance differences ( $*p < 0.05$ ) of the data within three replicated measurement ( $n = 3$ ).

plication on inducing cancer cell death, we performed apoptosis analysis through flow cytometry. HST and PGV-1 alone and its combination manifest apoptosis phenomenon under 10% for 24 h. The percentage of cells undergoing apoptosis is low due to the short incubation period. Therefore, we extended the incubation time of the apoptosis assay to 48 h. After 48 h, their combination exerted apoptotic cells in 21% (Figure 3b). The number of apoptotic cells was two times greater than that of the control. Furthermore, the combination of HST and PGV-1 increased cell death by modulating apoptosis at 48 h. The mechanism of apoptosis induction is associated with DNA damage. Damaged cells undergo senescence before regeneration. We conducted senescence tests to determine morphological cell changes due to the aging of cancer cells, especially luminal breast cancer.

### Cellular Senescence Effect

We explored the influence of HST and PGV-1 on inducing senescence in T47D using an assay involving associated  $\beta$ -galactosidase. Senescent cells were distinguished by the emergence of a green hue within the cells, indicating the presence of  $\beta$ -galactosidase expression (Figure 4a).

PGV-1 and HST alone increased  $\beta$ -galactosidase positive cells significantly by two up to three fold compared to the control. Interestingly, their combination showed two-fold induction of green cells than the single treatment (Figure 4b). These results indicate that combining PGV-1 and HST can increase cell senescence in T47D cells, where this pro-senescence effect is highly desirable in cancer. Pro-senescence activity

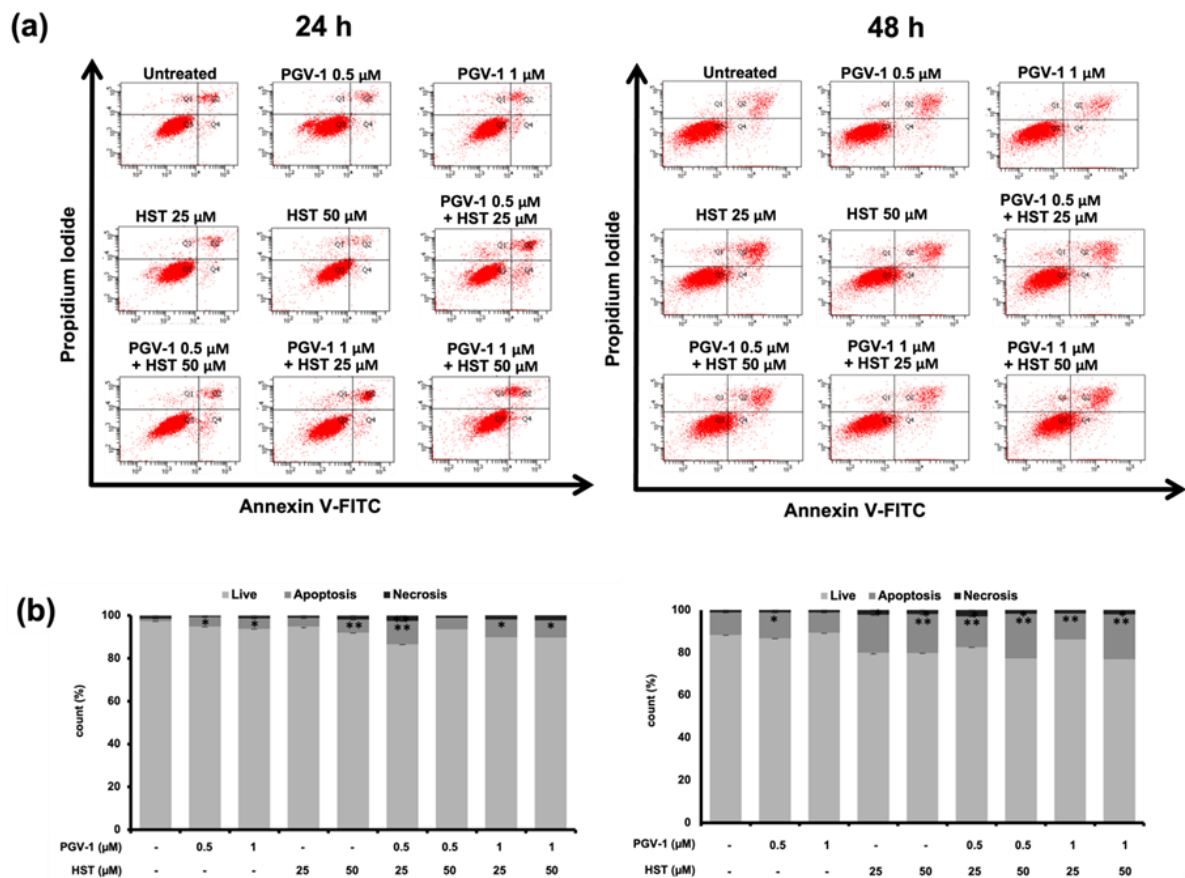


**Figure 3.** Apoptosis effects after treatment with PGV-1, HST, and their co-administration on T47D. Cells were subjected to PGV-1, HST, or both co-administration in various concentrations as indicated followed by 24 h incubation. After washing with cold PBS, the cells were stained with FITC Annexin V and Propidium Iodide, then subjected to flow cytometry. Apoptosis effects were generated from flow cytogram (a) into quantitative diagram (b) to obtain the significance differences ( $*p < 0.05$ ;  $**p < 0.001$ ) of the data within three replicated measurements ( $n = 3$ ).

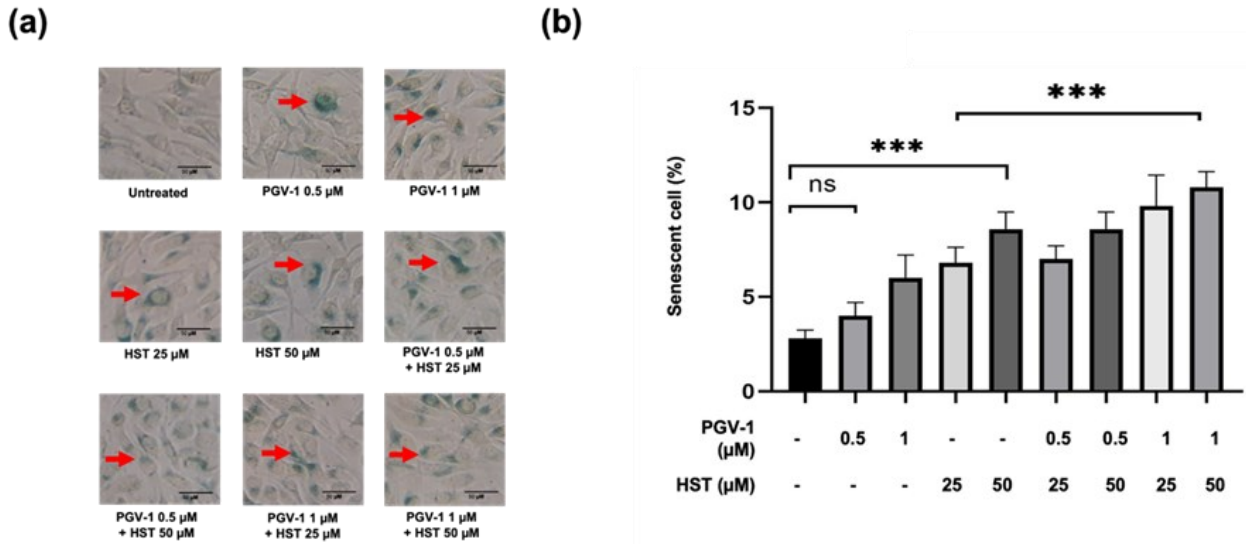


**Figure 4.** Senescent effects after treatment with PGV-1, HST, and their co-administration on T47D. Cells were subjected to PGV-1, HST, or both co-administration in various concentrations as indicated followed by 24 h incubation. They were stained using X-Gal. (a) Green color (red arrows) indicated cells stained with X-Gal hydrolyzed by  $\beta$ -galactosidase, expressed when cells were senescent. (b) The quantification of cellular senescence. The data are presented as average ( $n = 3$ ). ns, not significant; \*\*\* $p \leq 0.001$ .

demonstrated as a result of this treatment has a beneficial impact on inhibiting cancer cell development. However, further knowledge of its selectivity in normal cells is still needed to ensure its safety.

### HST attenuates DOX induced-normal cells senescence

We evaluated the cytotoxicity and senescent cell effects in NIH-3T3 normal fibroblasts and Vero normal kidney cells. We explored the cytotoxic effects of HST through the MTT assay. HST performs  $IC_{50}$  values of 700 μM and 314 μM in NIH-3T3 and Vero cells, respectively (Figure 5a). Consequently, HST was found to be non-toxic to Vero and NIH-3T3 cells.

Additionally, we evaluated the senescence effect of HST on both normal cells by using doxorubicin (DOX) as a cell senescence-inducing agent. DOX produced five times more green cells than green cells in control. Hence, DOX can serve as a positive reference for the senescence assessment (Figure 5b). The combination of DOX with HST of 50 and 100 μM reduced the number of green cells significantly with  $p$  value  $< 0.001$  compared to DOX alone. This response suggests that HST reduces intracellular senescent cells in NIH-3T3 and Vero cells.

## DISCUSSION

Hesperitin (HST) has long been used as a human health supplement to promote immunity, hormone balance, and inflammatory responses. Knowing the health response to HST, this study challenges its potential as a co-chemotherapeutic agent with PGV-1. The data showed that HST weakly suppressed the growth of T47D cells; however, when combined with PGV-1, HST escalated its cytotoxic effect synergistically. These results indicate that HST potentially enhances PGV-1 efficacy in luminal breast cancer cells by modulating its cytotoxic activity. This effect is probably triggered by differences in the molecular mechanisms of the two compounds.

In order to gain deeper insights into the impact of HST on cellular physiology, we examined the influence of HST alone and in co-



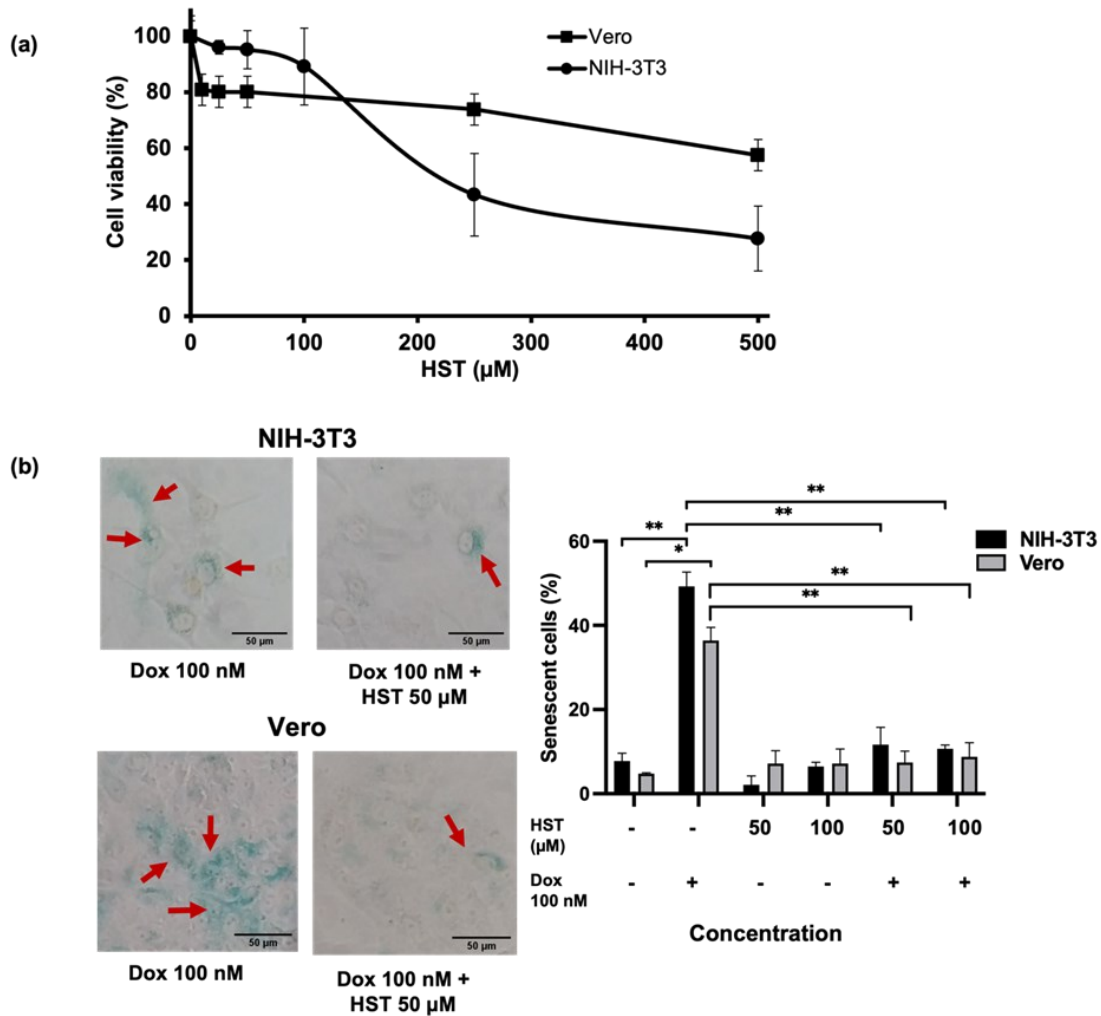


**Figure 5.** The effect of HST on NIH-3T3 and Vero. (a) Cell viability profile after treatment with drug followed by 24 h incubation. (b) Observation of senescence and its quantification in NIH-3T3 and Vero after being given HST. The results are shown as the mean ± SE for a total of three replicates. Dox: doxorubicin. \* $p < 0.05$ ; \*\* $p < 0.001$ .

administration with PGV-1 on the progression of the cell cycle. Remarkably, these combinations exhibited distinct targets for inhibiting the cell cycle. A concentration of 50 μM HST led to the arrest of the cell cycle at the G2/M phase within T47D. Notably, the co-administration of HST and PGV-1 triggered a more pronounced cell cycle halt at the G2/M phase, surpassing the effect of HST treatment alone. A similar effect was observed with a single HST administration in U937 cells (Lin et al. 2023). On the other hand, PGV-1 targets the M phase, specifically the prometaphase (Lestari et al. 2019; Meiyanto et al. 2022). The different target of cell cycle inhibition could result in strong cell growth inhibition and lead to apoptosis (Suski et al. 2021; Hanifa et al. 2022). In this regard, we found that HST elicited modulation of apoptosis of T47D cells at 48 h. Uniquely, HST also causes cell autophagy (Lin et al. 2023). Autophagy triggers the apoptotic response by activating caspase-8 and reducing anti-apoptotic proteins (Fan & Zong 2012). The simultaneous presence of apoptosis and autophagy can strengthen the effect of cancer cell death. We traced the events of cell death further by observing the morphology associated with the process of senescent cells.

Senescent cells become one of the strategic cancer inhibition targets because some cancer cells adapt by deactivating senescence signals (Hanahan & Weinberg 2011). Cell senescence is affected by the presence of cellular stress signals, such as DNA damage and under cellular abrogation (Huang et al. 2022). The concurrent application of HST and PGV-

1 led to a higher count of cells exhibiting senescence. In line with the results of this assay, we know that HST with PGV-1 modulates senescent cells, and this effect is positively correlated with increased inhibition of mitotic cells and cell death. Although the co-administration of these two compounds shows good molecular death effects on luminal breast cancer cells, tracing their cytotoxic activity on normal cells is necessary to ensure their efficacy and safety.

HST possesses strong antioxidant and immunomodulatory properties that hopefully can play a role as the normal cell protection from oxidative stress (Parhiz et al. 2015). For this purpose, we used NIH-3T3 cell line and vero cell line as the representative of skin and kidney tissues respectively, which are usually to be the riskiest tissue against cellular damaging agents (Endah et al. 2022). Our data reveal that individual HST application did not result in toxicity for either NIH-3T3 or Vero cells. Aligned with the outcomes of the cytotoxicity assessment, HST exhibited a reduction in the count of senescent cells induced by doxorubicin (DOX) in both normal cell types. We used DOX as the representative of strong senescent inducing-agents that have been known to cause cellular damage via Reactive Oxygen Species (ROS) generation (Salsabila et al. 2023). These results indicated that HST potentially protects against premature aging and damage to skin and kidney tissues. In this study, HST demonstrated its ability to increase the efficacy of PGV-1 and could help to protect surrounding cells from damage. In general, cell damage can be induced by oxidative agents including drugs, cellular stress, and poisons (Madkour 2020; Zulfin et al. 2021). These findings provide backing for the prospective development of HST as a co-chemotherapeutic agent, capable of enhancing the cytotoxic impact of chemotherapy agents and to reduce the cellular damages caused by toxic agents, including oxidative stress.

## **CONCLUSION**

In conclusion, HST synergistically enhanced PGV-1 efficacy by increasing its growth suppression effect against T47D as representative of luminal breast cancer. This phenomenon correlates to their inhibition of cell cycle machinery especially at mitosis, which leads to senescence and apoptosis. Treatment of HST in combination with PGV-1 may also protect cells from premature aging and prevent damage to kidney tissue. These results suggest the possibility of utilizing HST as a co-chemotherapeutic agent targeting luminal breast cancer, eliciting cell death.

## **AUTHORS CONTRIBUTION**

FNPR and UMZ conducted laboratory experiments and analyzed data; MH analyzed statistical data and prepared the manuscript; MI proofed outline and revised the manuscript; EM constructed the idea, organized and validated all data projects, and finalized the manuscript.

## **ACKNOWLEDGMENTS**

We thank the Cancer Chemoprevention Research Center (CCRC) for assisting in running the research and completing this manuscript. This publication is supported by the Rekognisi Tugas Akhir (RTA) program of UGM 2022. All these experiments are partially supported by the LPDP project 2021.

## **CONFLICT OF INTEREST**

The authors declare no conflicts of interest.

## REFERENCES

- Amalina, N.D. et al., 2023. In vitro synergistic effect of hesperidin and doxorubicin downregulates epithelial-mesenchymal transition in highly metastatic breast cancer cells. *Journal of the Egyptian National Cancer Institute*, 35(1), 6. doi: 10.1186/s43046-023-00166-3.
- Baghban, R. et al., 2020. Tumor microenvironment complexity and therapeutic implications at a glance. *Cell Communication and Signaling*, 18(1), 59. doi: 10.1186/s12964-020-0530-4.
- Burstein, H.J., 2020. Systemic Therapy for Estrogen Receptor-Positive, HER2-Negative Breast Cancer. *New England Journal of Medicine*, 383(26), pp.2557–2570. doi: 10.1056/NEJMra1307118.
- Čermák, V. et al., 2020. Microtubule-targeting agents and their impact on cancer treatment. *European Journal of Cell Biology*, 99(4), 151075. doi: 10.1016/j.ejcb.2020.151075.
- Choi, S.S., Lee, S.H. & Lee, K.A., 2022. A Comparative Study of Hesperitin, Hesperidin and Hesperidin Glucoside: Antioxidant, Anti-Inflammatory, and Antibacterial Activities In Vitro. *Antioxidants*, 11(8), 1618. doi: 10.3390/antiox11081618.
- Clusan, L. et al., 2023. A Basic Review on Estrogen Receptor Signaling Pathways in Breast Cancer. *International Journal of Molecular Sciences*, 24(7), 6834. doi: 10.3390/ijms24076834.
- Corrêa, T.A.F. et al., 2019. The Two-Way Polyphenols-Microbiota Interactions and Their Effects on Obesity and Related Metabolic Diseases. *Frontiers in Nutrition*, 6, 188. doi: 10.3389/fnut.2019.00188.
- Crescenti, A. et al., 2022. Hesperidin Bioavailability Is Increased by the Presence of 2S-Diastereoisomer and Micronization—A Randomized, Crossover and Double-Blind Clinical Trial. *Nutrients*, 14(12), 2481. doi: 10.3390/nu14122481.
- Endah, E. et al., 2022. Piperine Increases Pentagamavunon-1 Anti-cancer Activity on 4T1 Breast Cancer Through Mitotic Catastrophe Mechanism and Senescence with Sharing Targeting on Mitotic Regulatory Proteins. *Iranian Journal of Pharmaceutical Research*, 21(1), e123820. doi: 10.5812/ijpr.123820.
- Fan, Y.J. & Zong, W.X., 2012. The cellular decision between apoptosis and autophagy. *Chinese Journal of Cancer*, 32(3), pp.121–129. doi: 10.5732/cjc.012.10106.
- Filho, I.K. et al., 2021. Optimized Chitosan-Coated Gliadin Nanoparticles Improved the Hesperidin Cytotoxicity over Tumor Cells. *Brazilian Archives of Biology and Technology*, 64(spe), e21200795. doi: 10.1590/1678-4324-75years-2021200795
- Hanahan, D. & Weinberg, R.A., 2011. Hallmarks of Cancer: The Next Generation. *Cell*, 144(5), pp.646–674. doi: 10.1016/j.cell.2011.02.013.
- Hanifa, M. et al., 2022. Different Cytotoxic Effects of Vetiver Oil on Three Types of Cancer Cells, Mainly Targeting CNR2 on TNBC. *Asian Pacific Journal of Cancer Prevention*, 23(1), pp.241–251. doi: 10.31557/APJCP.2022.23.1.241.
- Haque, A., Brazeau, D. & Amin, A.R., 2021. Perspectives on natural compounds in chemoprevention and treatment of cancer: An update with new promising compounds. *European Journal of Cancer*, 149, pp.165–183. doi: 10.1016/j.ejca.2021.03.009.
- Hasbiyani, N.A.F. et al., 2021. Bioinformatics Analysis Confirms the Target Protein Underlying Mitotic Catastrophe of 4T1 Cells under Combinatorial Treatment of PGV-1 and Galangin. *Scientia Pharmaceutica*, 89(3), 38. doi: 10.3390/scipharm89030038.

- Heery, A. et al., 2020. Precautions for Patients Taking Aromatase Inhibitors. *Journal of the Advanced Practitioner in Oncology*, 11(2), pp.184–189. doi: 10.6004/jadpro.2020.11.2.6.
- Huang, W. et al., 2022. Cellular senescence: The good, the bad and the unknown. *Nature Reviews Nephrology*, 18(10), pp.611–627. doi: 10.1038/s41581-022-00601-z.
- Ikawati, M. et al., 2023. The Synergistic Effect of Combination of Pentagamavunone-1 with Diosmin, Galangin, and Piperine in WiDr Colon Cancer Cells: *In vitro* and Target Protein Prediction. *Journal of Tropical Biodiversity and Biotechnology*, 8(2), 80975. doi: 10.22146/jttb.80975.
- Lee, H.J & Choi, C.H., 2022. Characterization of SN38-resistant T47D breast cancer cell sublines overexpressing BCRP, MRP1, MRP2, MRP3, and MRP4. *BMC Cancer*, 22(1), 446. doi: 10.1186/s12885-022-09446-y.
- Lestari, B. et al., 2019. Pentagamavunon-1 (PGV-1) inhibits ROS metabolic enzymes and suppresses tumor cell growth by inducing M phase (prometaphase) arrest and cell senescence. *Scientific Reports*, 9(1), Article 1. doi: 10.1038/s41598-019-51244-3.
- Lin, C.Y, Chen, Y.H. & Huang, Y.C., 2023. Hesperitin Induces Autophagy and Delayed Apoptosis by Modulating the AMPK/Akt/mTOR Pathway in Human Leukemia Cells In Vitro. *Current Issues in Molecular Biology*, 45(2), pp.1587–1600. doi: 10.3390/cimb45020102.
- Madkour, L.H., 2020. Oxidative stress and oxidative damage-induced cell death. In *Reactive Oxygen Species (ROS), Nanoparticles, and Endoplasmic Reticulum (ER) Stress-Induced Cell Death Mechanisms*, pp.175–197. doi: 10.1016/B978-0-12-822481-6.00008-6.
- Masoud, V. & Pagès, G., 2017. Targeted therapies in breast cancer: New challenges to fight against resistance. *World Journal of Clinical Oncology*, 8(2), 120. doi: 10.5306/wjco.v8.i2.120.
- Meiyanto, E., Hermawan, A. & Anindyajati, A., 2012. Natural Products for Cancer-Targeted Therapy: Citrus Flavonoids as Potent Chemopreventive Agents. *Asian Pacific Journal of Cancer Prevention*, 13(2), pp.427–436. doi: 10.7314/APJCP.2012.13.2.427.
- Meiyanto, E. & Larasati, Y.A., 2019. The Chemopreventive Activity of Indonesia Medicinal Plants Targeting on Hallmarks of Cancer. *Advanced Pharmaceutical Bulletin*, 9(2), pp.219–230. doi: 10.15171/apb.2019.025.
- Meiyanto, E. et al., 2019. Anti-proliferative and Anti-metastatic Potential of Curcumin Analogue, Pentagamavunon-1 (PGV-1), Toward Highly Metastatic Breast Cancer Cells in Correlation with ROS Generation. *Advanced Pharmaceutical Bulletin*, 9(3), pp.445–452. doi: 10.15171/apb.2019.053.
- Meiyanto, E. et al., 2022. Bioinformatic and Molecular Interaction Studies Uncover That CCA-1.1 and PGV-1 Differentially Target Mitotic Regulatory Protein and Have a Synergistic Effect against Leukemia Cells. *Indonesian Journal of Pharmacy*, 33(2), pp.225–233. doi: 10.22146/ijp.3382.
- Mueller, M. et al., 2018. Rhamnosidase activity of selected probiotics and their ability to hydrolyse flavonoid rhamnoglucosides. *Bioprocess and Biosystems Engineering*, 41(2), pp.221–228. doi: 10.1007/s00449-017-1860-5.
- Musyayyadah, H. et al., 2021. The Growth Suppression Activity of Diosmin and PGV-1 Co-Treatment on 4T1 Breast Cancer Targets Mitotic Regulatory Proteins. *Asian Pacific Journal of Cancer Prevention*, 22(9), pp.2929–2938. doi: 10.31557/APJCP.2021.22.9.2929.

- Novitasari, D. et al., 2021. CCA-1.1, a Novel Curcumin Analog, Exerts Cytotoxic anti- Migratory Activity toward TNBC and HER2-Enriched Breast Cancer Cells. *Asian Pacific Journal of Cancer Prevention*, 22(6), pp.1827–1836. doi: 10.31557/APJCP.2021.22.6.1827.
- Nurhayati, A.P.D. et al., 2019. The phagocytosis activity of isoeugenol-ester compound on *Mus musculus* macrophage cell. *Nusantara Bioscience*, 11(2), Article 2. doi: 10.13057/nusbiosci/n110201.
- Parhiz, H. et al., 2015. Antioxidant and Anti-Inflammatory Properties of the Citrus Flavonoids Hesperidin and Hesperetin: An Updated Review of their Molecular Mechanisms and Experimental Models. *Phytotherapy Research*, 29(3), pp.323–331. doi: 10.1002/ptr.5256.
- Putri, D.D.P. et al., 2022. Acute toxicity evaluation and immunomodulatory potential of hydrodynamic cavitation extract of citrus peels. *Journal of Applied Pharmaceutical Science*, 12(4), pp.136–145. doi: 10.7324/JAPS.2022.120415.
- Salsabila, D. et al., 2023. Cytoprotective Properties of Citronella Oil (*Cymbopogon nardus* (L.) Rendl.) and Lemongrass Oil (*Cymbopogon citratus* (DC.) Stapf) through Attenuation of Senescent-Induced Chemotherapeutic Agent Doxorubicin on Vero and NIH-3T3 Cells. *Asian Pacific Journal of Cancer Prevention*, 24(5), pp.1667–1675. doi: <https://doi.org/10.31557/APJCP.2023.24.5.1667>.
- Suski, J.M. et al., 2021. Targeting cell-cycle machinery in cancer. *Cancer Cell*, 39(6), pp.759–778. doi: 10.1016/j.ccell.2021.03.010.
- Takumi, H. et al., 2012. Bioavailability of orally administered water-dispersible hesperitin and its effect on peripheral vasodilatation in human subjects: Implication of endothelial functions of plasma conjugated metabolites. *Food & Function*, 3(4), 389. doi: 10.1039/c2fo10224b.
- Utomo, R.Y. et al., 2022. Preparation and Cytotoxic Evaluation of PGV-1 Derivative, CCA-1.1, as a New Curcumin Analog with Improved-Physicochemical and Pharmacological Properties. *Advanced Pharmaceutical Bulletin*, 12(3), pp.603–612. doi: 10.34172/apb.2022.063.
- Wdowiak, K. et al., 2022. Bioavailability of Hesperidin and Its Aglycone Hesperitin—Compounds Found in Citrus Fruits as a Parameter Conditioning the Pro-Health Potential (Neuroprotective and Anti-diabetic Activity)—Mini-Review. *Nutrients*, 14(13), 2647. doi: 10.3390/nu14132647.
- Zulfin, U. et al., 2021. Reactive oxygen species and senescence modulatory effects of rice bran extract on 4T1 and NIH-3T3 cells co-treatment with doxorubicin. *Asian Pacific Journal of Tropical Biomedicine*, 11(4), 174. doi: 10.4103/2221-1691.310204.